

This document has been approved for public release and sale; its distribution is unlimited.

RR79004

MINISTRY OF DEFENCE

LEVEL II

①

ROYAL ARMAMENT RESEARCH AND DEVELOPMENT ESTABLISHMENT

DTIC ELECTE
SEP 14 1981
S E D

RARDE TECHNICAL REPORT 2/81

Contrast Discrimination by the Human Visual System

G.J. Burton

The information given in this document is not to be communicated either directly or indirectly to the Press or to any person not authorised to receive it.

**Fort Halstead
Kent**

**May
1981**

81 8 19 023

2/81

AD A104181



DTIC FILE COPY

IMPORTANT

This document should be returned to the Reports Officer, Royal Armament Research and Development Establishment, Fort Halstead, Sevenoaks, Kent, when no longer required

This Document was Graded
- Unclassified
at the 363 meeting of the R.A.R.D.E.
Security Classification Committee

- 1. T
G
- 2. T
P
- 3. T

A
ENT

EMENTS
S WITHIN ITS
TY OF
INFORMATION

- 4.
- 5.

E TREATED
L USE ITS
T WITH IN
REOF TO

OBTAIN PATENT OR OTHER STATUTORY PROTECTION THEREFOR.

- 6. BEFORE ANY USE IS MADE OF THIS INFORMATION FOR THE PURPOSE OF MANUFACTURE, THE AUTHORISATION OF THE MINISTRY OF DEFENCE MUST BE OBTAINED.

MINISTRY OF DEFENCE

(18) DRIC

ROYAL ARMAMENT RESEARCH AND DEVELOPMENT ESTABLISHMENT9
RARDE TECHNICAL REPORT 2/81

(19) BR-79004

(6) Contrast Discrimination by the Human Visual System.

(10) G.J. Burton PhD, MInstP

(11) May 87

(14) RARDE-TR-2/87

(12) 32

Summary

In vision of everyday scenes, features requiring detection are frequently observed in the presence of suprathreshold background structures. Detection of such features is a contrast discrimination task and is often necessary for the subsequent process of recognition. In order to provide a description of this task, contrast discrimination measurements were determined for targets with luminance profiles which were localised in both space and spatial frequency. The investigation extends earlier work on this topic by measurement of contrast discrimination levels for different base contrasts, sizes, luminances, and aspect ratios of the targets. A model is proposed to describe the contrast discrimination process, and an example is given of a simple application of the model to the determination of the number of discriminable steps in contrast as a function of the spatial frequency of a sinusoidal grating target.

Approved for issue:

G. H. Cockett
G H Cockett
Head of Applied Physics Department

Reprint with minor amendments of a paper published in Biological Cybernetics, Vol 34, 1981.

UNCLASSIFIED

CONTENTS

	Page
1 Introduction	3
2 Methods	4
3 Results	6
4 Discussion	15
5 Conclusions	20
6 References	21
Annex Theoretical Model of Contrast Discrimination	A-2

Accession For	
NTIS GRA&I	
DTIC TAB	
Unannounced	
Justification	
By	
Distribution	
Availability Codes	
Dist	Avail and/or Special
A	

1 INTRODUCTION

This report is the first in a planned series concerning work which is primarily directed at describing visual performance with imaging systems.

Much research in spatial vision has been concerned with the measurement and modelling of performance levels for the detection of structures presented on uniform background fields. On the basis of the lead given by Schade (Ref 1), many experiments have been designed around a linear systems analogy, and as such have used sinusoidal gratings as stimuli in order to define some assumed fundamental responses of spatial vision (Refs 2,3). The signal transfer function of the system is taken to be linear for small signal amplitudes. At a given ambient light level, it is assumed that the visual system can be represented by a single spatial filter: a single-channel model. However, there is considerable evidence that several mechanisms may mediate threshold detection leading to the formulation of multiple-channel models (Refs 4-7). In addition, the assumption that the contrast sensitivity function, as derived from detection threshold levels of sinusoidal gratings, represents a modulation transfer function in the conventional sense has been questioned (Refs 8-10). Such studies show that the band-pass attribute of the spatial frequency response function becomes progressively less frequency selective as contrast increases (Refs 11-13), as if apparent contrast is equal to physical contrast minus contrast threshold. A process of neural 'deblurring' has been proposed by Georgeson & Sullivan (Ref 8) to explain this effect. Snyder and Srinivasan (Ref 14) consider a more general interpretation in which the visual system compensates for both optical degradation and noise contamination in the signal to noise discrimination task. A non-linear signal transfer function of the decelerating type (eg logarithmic) will cause the apparent contrasts of gratings of all spatial frequencies to tend towards equality (Ref 15), though this behaviour is not consistent with the contrast linearity observed by Cannon (Ref 10).

Suprathreshold contrast measurements seem to be at variance with data from single-cell recordings which can show spatial frequency dependent (suprathreshold) responses at most stages throughout the primary visual pathway (Refs 16-18). This may mean that significant spatial processing occurs at levels more central than those as yet examined by single-cell recording, that populations of cells presumably active in psycho-physical experiments have mass properties which are not readily derived from single-cell responses, or possibly that some cell response other than spike frequency is the critical parameter (eg the statistics of the relationship between individual spikes (Ref 19).

In spite of the evidence which reveals flaws in the general applicability of single-channel models of spatial vision, such models have been widely used in the design of imaging devices, especially electro-optic systems. This is presumably because such models capture the essence of spatial vision in that they provide a decreasing response as spatial frequency increases (which implies an acuity limit), and give a poor response to diffuse targets. In addition the models have a simple construction and are fast in application.

Models consisting of several channels are necessary in order to embrace the effects on detection threshold levels of subthreshold structures (Refs 6,7) and masking background fields (Refs 20, 21). Such models are consistent with much experimental evidence (Refs 22-25). In vision of everyday scenes, however, features requiring detection are often observed in the presence of suprathreshold background structures. The detection of such features is necessary for the process of recognition. Therefore a description of suprathreshold vision is not only useful for specifying the appearance of objects (cosmetic quality) but also crucial for determining those features of an object which are available for subsequent recognition by the trained higher brain: the primal sketches of Marr (Ref 26).

Assuming that magnitude estimation (Ref 10) and contrast halving (Ref 9) provide correct descriptions of signal transfer functions in spatial vision, it seems that perceived contrast is equal to objective contrast minus contrast threshold. If in addition the statistical spread of suprathreshold responses is known for a fixed target contrast, then a first step can be made towards modelling suprathreshold spatial vision. Such a model can be applied to several problems: the prediction of just-noticeable differences in measures of image quality (eg system MTF); the accuracy of visual accommodation required to avoid loss of image quality (Ref 27); and the design of digital image coding, transmission and displays systems in which luminance levels are quantised and interact with spatial sampling intervals (Refs 28-32).

The aim of the present investigation is to measure contrast discrimination levels for different contrasts, etc, sizes, luminances and aspect ratios of targets with triphasic spatial profiles (Fig 1a). Such targets are localised in both space and spatial frequency, so avoiding probability summation effects (Refs 25, 33, 34) while retaining moderate spatial frequency selectivity. The investigation extends the results of Nachmias & Sansbury (Ref 35), Kohayakawa (Ref 36) and Kulikowski (Ref 9). A further aim was to place on a firm experimental basis assumptions made by Mezrich, Carlson & Cohen (Ref 30) in their calculations of the theoretical number of grey scale steps as a function of spatial frequency, and the minimum number of bits required for faithful image reproduction on displays.

2 METHODS

Targets were generated by a Microconsultants INTELLECT framestore and image processing system controlled by a Computer Automation LSI-2 computer. The frame store has a resolution of 512x512 picture elements (pixels) with an 8-bit grey scale. Output from the framestore drives a digital to analogue converter at 50Mbit/sec enabling targets to be displayed on a broadcast quality monitor (PYE TVT Model LDM15 fitted with a green (GH) phosphor; chromaticity coordinates $x=0.270$, $y=0.602$). The observer viewed the display from a range of 3.5m with his head resting in a close fitting support. At this range the screen subtended 4.7 deg horizontal and 3.2 deg vertical. The pixel subtense was 0.55min horizontal and 0.375min vertical. A rectangular, uniform surround field (14.7deg horizontal, 10.8deg vertical) was provided by means of mat, white card and a projector with an interposed filter solution made from cupric chloride and potassium

produce an approximate match to the colour and luminance of the monitor display. The monitor luminance was set at 28cd.m^{-2} . In order to maintain this value of luminance the monitor AC supply was provided by a Cintec voltage and frequency stabilizer. Lower luminance values were achieved by placing large neutral filters (titanium on glass) close to the eyes of the observer. The experiments required the presentation of contrasts ranging from about 0.001 to 0.8 (equation 1). By selecting different settings of the monitor brightness and contrast controls, while maintaining constant mean luminance, three overlapping contrast scales were obtained. Thus sufficient luminance resolution was retained in the mapping from the frame store grey scale. Each contrast scale was calibrated using a Gamma Scientific telephotometer, model 2009. Appropriate non-linear corrections were applied so that the contrast as specified in the controlling computer program was the same as that which appeared on the monitor.

Most values of contrast discrimination were obtained by using a two-alternative forced-choice paradigm designed to achieve a 71% probability of correct discrimination between two targets of different contrast. Coded tones indicated correct and incorrect responses. (Methods employing 'same' or 'different' responses were tried but were found to be unreliable because nominally identical targets, other than point sources, almost always appear different during a given presentation owing to random point-to-point fluctuations in visual responses.) Values of contrast were presented by using a randomly interleaved, double staircase procedure (Ref 38) with adaptive steps (Ref 39) so that the region of 71% correct discrimination was achieved rapidly with large contrast steps, leading to small contrast steps as the threshold value became more localised. A number of preliminary presentations (typically 40) were made, until the step size in contrast difference for both staircases fell below 20%. After this point 40 further presentations occurred. The final value of contrast discrimination was determined by averaging the 40 values of contrast difference for both staircases. In order to determine the experimental errors appropriate to this procedure, some double staircase procedures were repeated 10 times. Standard deviations of contrast discrimination were obtained by this method.

The main experiments used side-by-side presentation of the two targets. The observer was instructed to direct his gaze from one target to the other during the 2 second presentation and ignore on and off transients. The centre-to-centre target separation was 0.92deg for all triphasic targets except for the largest target used (centre bar width 35min) for which the separation was increased to 1.84deg . The interval between target presentations was at least 3s during which time the observer viewed a uniform field. A small dark reference cross or spot was provided in the centre of the monitor field in order to aid target location for near or below threshold targets. Side-by-side presentation of targets was used in preference to temporal forced-choice methods since the former relies less on memory and more closely resembles the type of comparison of image quality often employed in system design. However, a short experiment was performed using temporal forced-choice presentation: first target on for 2s, uniform field for 1s, second target on for 2s, then a delay of at least 3s before presentation of the next pair of targets.

UNCLASSIFIED

Most experiments used triphasic targets consisting of a central bar flanked by two bars of opposite sign (contrast profiles are shown in Fig 1a). The examples in Figure 1a show positive triphasic profiles: a central bright bar flanked by dark bars. The alternative polarity of target (negative triphasic) was also used. The targets are more localised than the grating patches employed by Graham, Robson and Nachmias (Ref 34) and therefore some spatial frequency selectivity is lost, though the targets are more typical of the structures encountered in real objects. The continuous lines in Figure 1a are records of luminance obtained directly from the monitor screen using a Gamma Scientific photometric microscope, model 700-10 with 75 μ slit. The fine structure displayed in the scans is due to phosphor granularity. The open symbols describe the contrast values calculated in the experimental computer program with a small scaling correction applicable at high spatial frequencies (30c/deg) to account for the roll-off in whole system response. This reduced response is evident for the narrow targets shown in Figure 1a. Target width for triphasic profiles is defined as the width of the central bar, ie the distance between the two zero contrast crossings. Target contrast is specified by:

$$C = |L - L_0| / L_0 \quad (1)$$

where L is the luminance of the middle of the central bar and L_0 is the background luminance. For a positive triphasic profile of unit width and contrast, the equation describing the profile as a function of the spatial coordinate $0 < |x| < 1.305$ is:

$$C(x) = 1 - 1.829x - 1.073x^2 + 1.447x^3 \quad (2)$$

The modulus of the Fourier transform of the function for a target of size $D=4.4$ min and contrast 1.0 is shown by the open symbols in Figure 1b. A similar transformation of data from a photometric microscope scan of the monitor is described by the continuous line in Figure 1b. The good agreement between theoretical and experimental data in Figures 1a and 1b provides a useful check on equipment reliability. For a target of width D min the maximum F_m in the corresponding spatial frequency spectrum is:

$$F_m = 0.50/D \text{ c/min} \quad (3)$$

Two observers participated in the experiments: EM aged 43 and GJB aged 30. EM viewed the display binocularly and was not informed of the aims and procedures of the experiments. GJB, the author, viewed with the right eye only, the left eye being occluded. No artificial pupils or spectacle corrections were employed.

3 RESULTS

All measurements of contrast discrimination relate to the observation of one target of contrast, $C+\Delta C$, which can be chosen with some probability P as being of higher contrast than a similar target of base contrast C. Except for the data shown in Figure 9, the probability of a correct contrast choice in all experiments is approximately 0.71. The conventional contrast threshold for a given target therefore corresponds to the condition $C=0$. The targets used were always positive, triphasic profiles

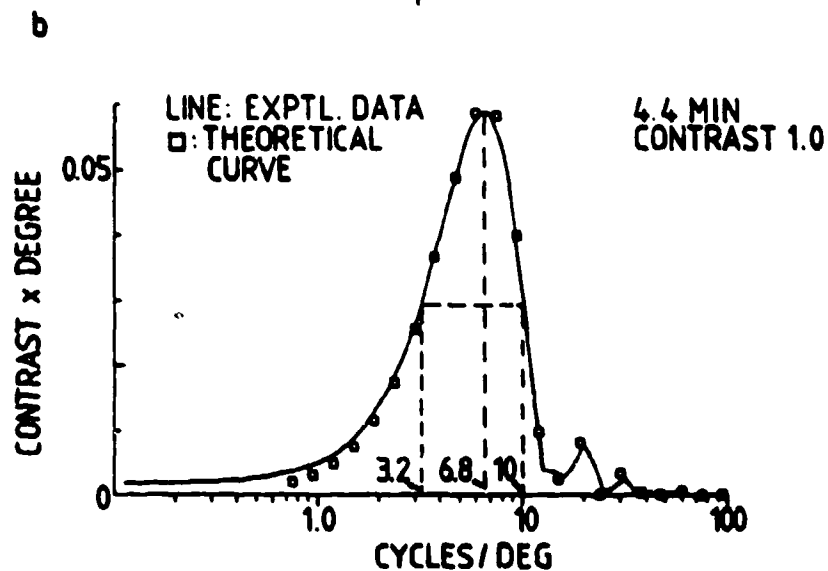
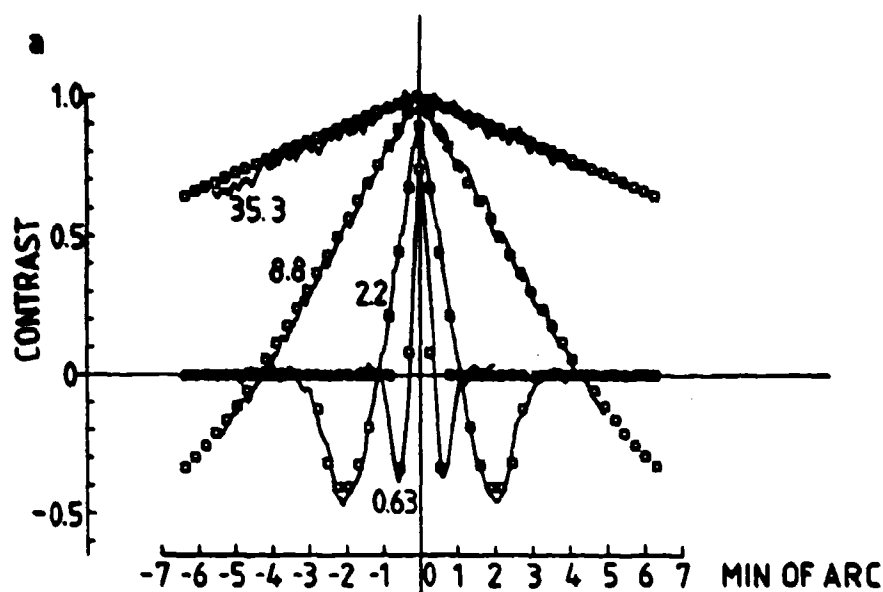


FIG 1(a) Continuous lines show photometric microscope scans of some triphasic profiles employed in the experiments. The open symbols represent the corresponding values as defined in the controlling computer program. Each target has a nominal contrast of 1.0 and the number adjacent to each curve defines the particular target width, min of arc, as specified by the width of the central (bright) bar. The microscope can scan an angle of only 13 min of arc: therefore the flanks of the two larger profiles are not plotted. The small reduction in contrast for the narrowest profile is due to a roll-off in whole system MTF at high spatial frequencies.

(b) Modulus of the Fourier transforms for experimental and theoretical triphasic profiles of width 4.4min. The total width between half maximum points is 1.6 octaves.

(Fig 1a) except where identified as negative, triphasic profiles or as linear sinusoidal gratings. All targets were orientated vertically and extended the full height of the display 3.2deg, except where the effect of different aspect ratios was examined. The mean display luminance was 28cd.m^{-2} for most experiments. In some figures error bars are shown which represent $\pm 1\text{sd}$ ($N=10$).

Conventional contrast threshold values for both observers are shown in Figure 2, values are determined for different target sizes. The 'band-pass' type of behaviour as observed for similar measurements with sinusoidal gratings is apparent, as is a 'cut-off' in the region of 0.01deg (approximately equivalent to a grating of spatial frequency of 50c/deg). These results lend support to the statement made earlier: the triphasic targets have a sufficiently selective spatial frequency content to produce visual responses similar to those of sinusoidal gratings without the associated difficulties produced by the presence of multiple cycles (Ref 33).

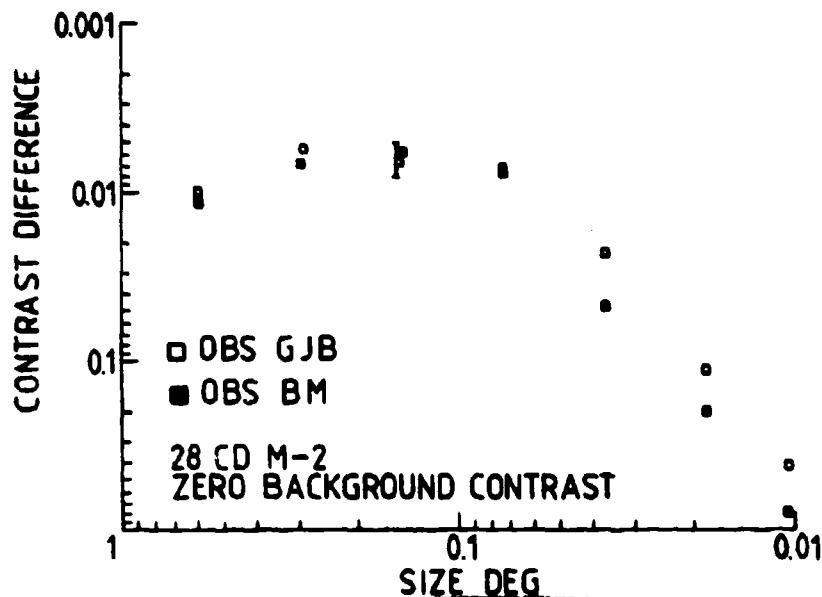


FIG 2 Conventional contrast threshold values for positive triphasic profiles of different widths. Filled and open symbols show data for Observers BM and GJB respectively. Luminance 28cd.m^{-2} .

Measurements of contrast difference ΔC determined for different values of base contrast C are shown in Figures 3a,b&c. A comparison of different experimental techniques is shown in Figure 3a, different polarities of triphasic profile in Figure 3b and different target types (triphasic profile and grating) in Figure 3c. In all cases, the contrast difference ΔC initially decreases for increasing base contrast C , and finally increases in a way which exhibits an approximate linearity of ΔC against C : the contrast Weber-Fechner region. Overall, the type of variation of ΔC with C is the same as that observed by Campbell & Kulikowski (Ref 40) and by Nachmias & Sansbury (Ref 35). The initial decrease in contrast difference ΔC has been termed subthreshold addition (Ref 6). The minimum value of ΔC (Fig 3) occurs at a value of base contrast C which is in the region of the conventional threshold level for the target.

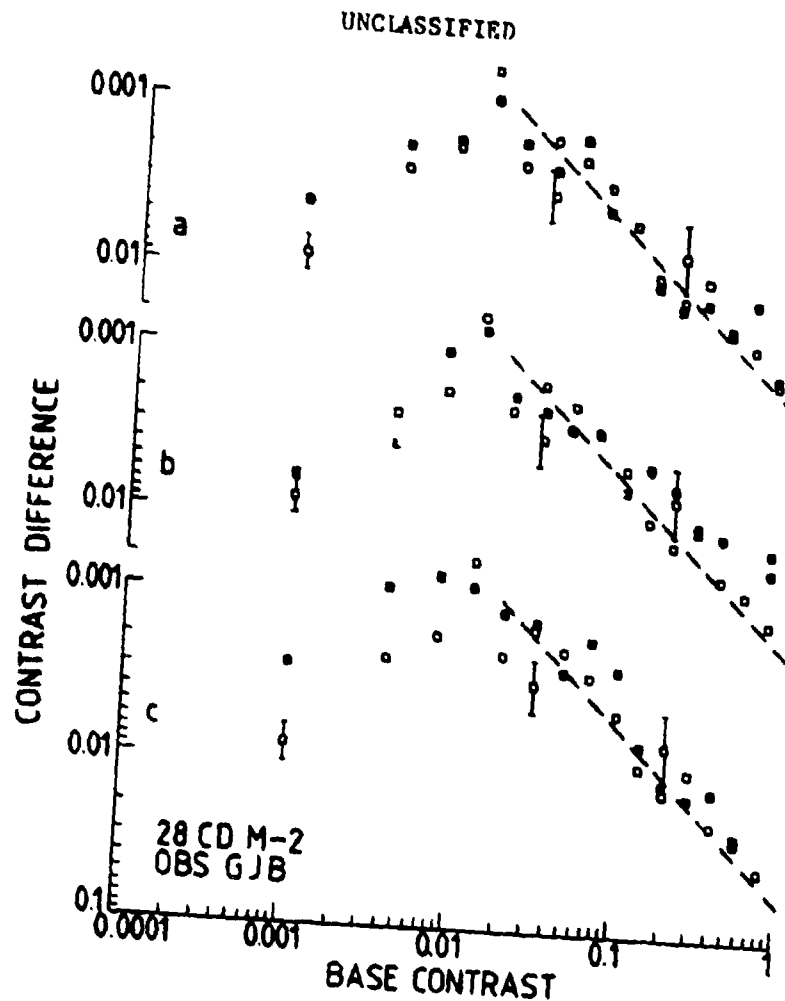


FIG 3 Comparison of contrast difference thresholds using various experimental techniques and targets. The broken lines have a slope of 1.0 with a contrast Weber-Fechner fraction of 0.055. Observer GJB, luminance 28cd.m^{-2} .

(a) Values obtained for positive triphasic targets by the methods of side-by-side forced-choice (open symbols) and temporal forced-choice (filled symbols), target width 0.15deg.

(b) The effect of different contrast polarities on contrast discrimination. Data for positive and negative triphasic profiles are shown by open and filled symbols respectively. Target width 0.15deg, side-by-side forced-choice method.

(c) Comparison of values obtained for a positive triphasic target, width 0.15deg (open symbols) and an equivalent sinusoidal grating, spatial frequency 3.4c/deg (filled symbols). Side-by-side forced-choice method.

Figures 4a&b show the effect of different target widths on the variation of contrast difference ΔC with base contrast C . The general trend of the results for each target width is similar to that shown in Figure 3 except that the placement of each set depends on the target width: each set shifts neither vertically nor horizontally but seems to slide along a 45deg line, so that when the base contrast C is sufficiently above threshold for a given target width, values of ΔC become approximately independent of the target width.

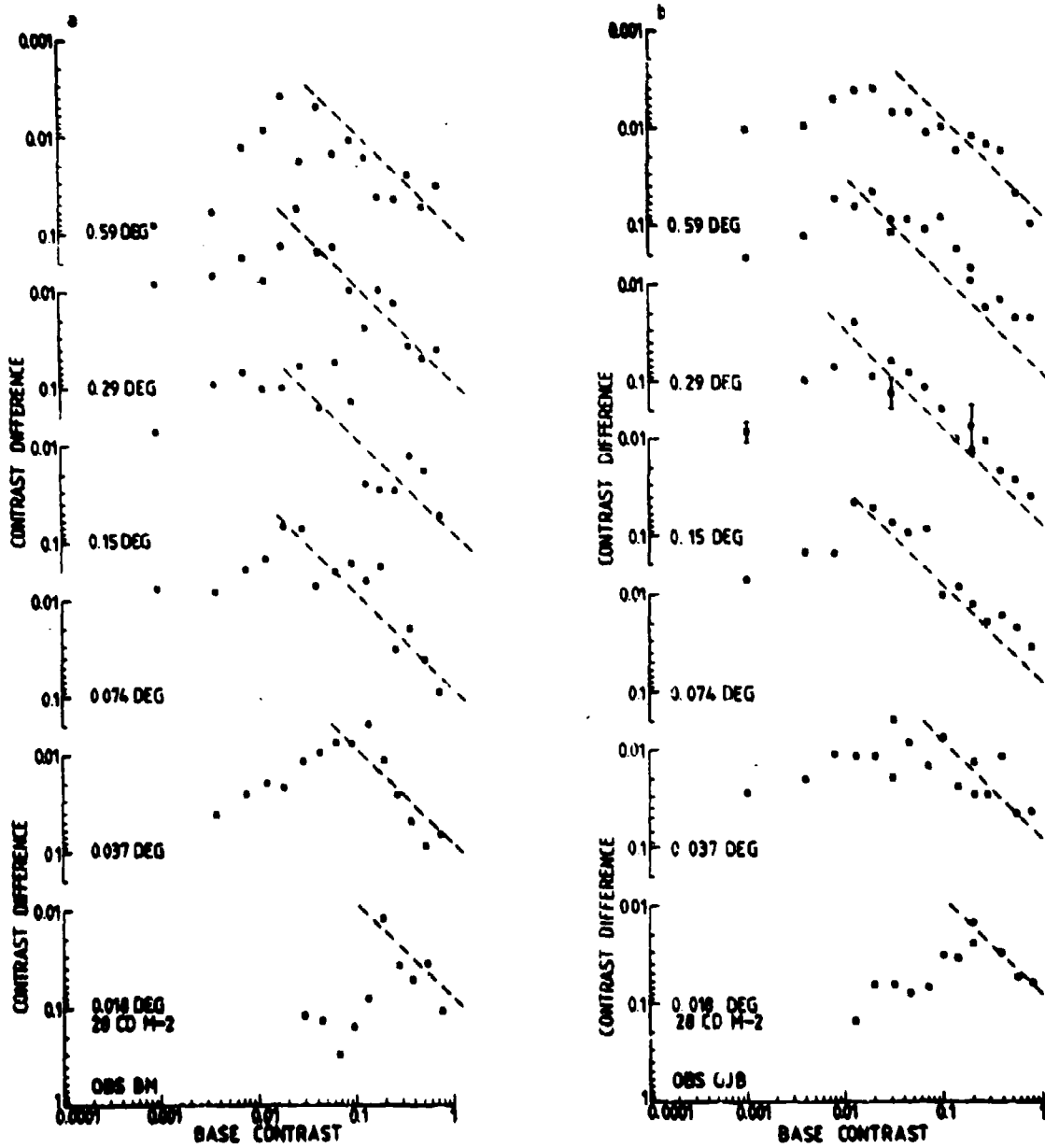


FIG 4 Contrast discrimination values obtained for different widths of triphasic targets. (a) Observer EM, (b) Observer GJB. Values were obtained by the method of side-by-side forced-choice using positive triphasic profiles. The dashed lines are drawn with a slope of 1.0 and contrast Weber-Fechner fraction of 0.08. The latter value is an average estimate of the fraction as shown in Figure 7. Luminance 28cd.m⁻².

The target of width 0.15deg was selected and used to determine the dependence of contrast discrimination on the display luminance. Values for one observer are shown in Figure 5. For each luminance the variation of contrast difference ΔC with base contrast C has similar characteristics to those already observed for the influence of target width (Fig 4). Thus each set of symbols moves along a 45deg line so that the placement of the set depends only on the conventional threshold level.

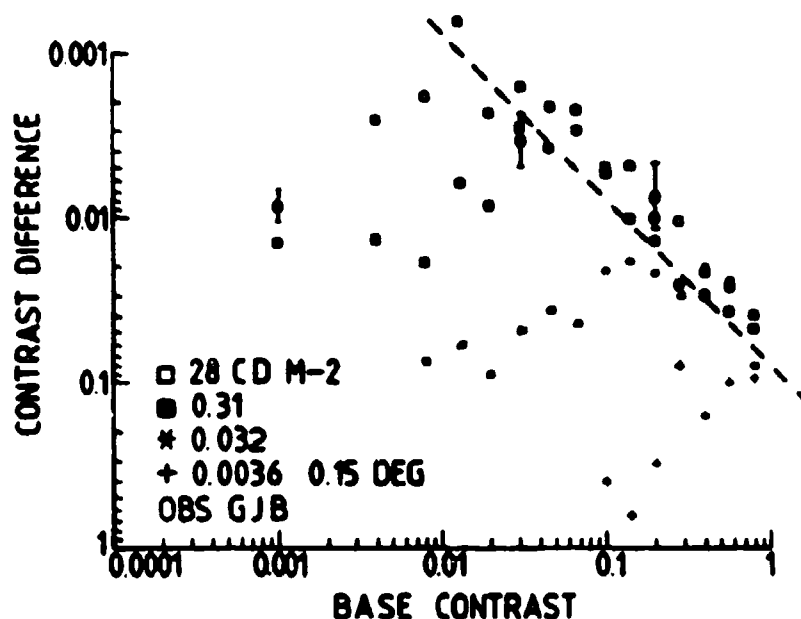


FIG 5 The influence of luminance on contrast discrimination of positive triphasic targets using the side-by-side forced-choice method. Values were obtained for luminances of 28, 0.31, 0.032 and 0.0036cd.m⁻² and are denoted by open squares, filled squares, asterisks and crosses respectively. Observer GJB, target width 0.15deg. The broken line is drawn with a slope of 1.0 and a contrast Weber-Fechner fraction of 0.08.

It is clear from the results shown in Figures 4&5 that, to a first approximation, values of ΔC in the contrast Weber-Fechner region are independent of the conventional threshold values when those values are altered by changing either the target width or the mean luminance.

The effect of different aspect ratios of the target (length/width) was briefly examined by determining the minimum detectable contrast difference for a target of width 0.15deg and contrast 0.8 as aspect ratio varied from the maximum attainable for this target width, 21.3 down to 1.0. Values for both observers are shown in Figure 6. There is no systematic variation of contrast difference ΔC with aspect ratio.

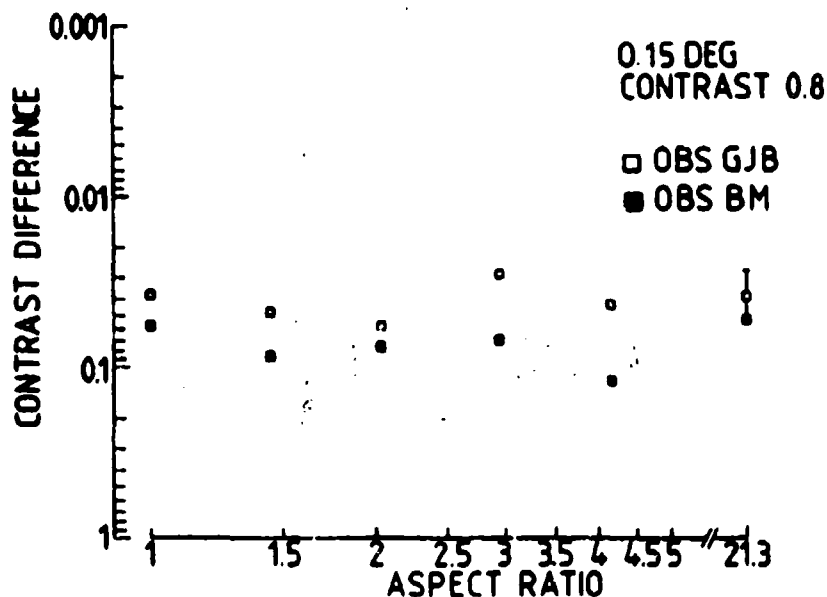


FIG 6 Illustrates that the length of a triphasic profile does not significantly affect the level of contrast discrimination when the base contrast is within the Weber-Fechner region. Filled symbols and open symbols show data for Observers BM and GJB respectively. Base contrast 0.8, target width 0.15deg and luminance $28\text{cd}\cdot\text{m}^{-2}$. Method of side-by-side forced-choice using positive triphasic targets.

It has been shown that the contrast difference ΔC is approximately proportional to the base contrast C for values somewhat greater than the conventional threshold level (Figs 2-5). The constant of proportionality W in the relationship $\Delta C = W \cdot C$ is defined as the contrast Weber-Fechner fraction. Values of W were estimated from the data shown in Figures 4a,b and are plotted against target width in Figure 7 for both observers (square symbols). Also shown is the value for negative triphasic targets as estimated from the data shown in Figure 3b. It is apparent that the contrast Weber-Fechner fraction W varies slowly with target size. Nevertheless, a mean value of W , 0.08, was calculated by averaging over the data for both observers and all widths, because such a 'single-number' provides a useful designer's rule-of-thumb and is a sufficiently accurate representation for many practical situations. A value of W was also estimated from the data given by Nachmias & Sansbury (Ref 35). This single value, determined for a grating of spatial frequency 3c/deg, is plotted in terms of the equivalent triphasic bar width. Since the experimental technique employed by Nachmias & Sansbury is similar to that used in the present investigation, the magnitude of the difference between this single value and the values obtained in this investigation is sufficiently large to justify the averaging process used to derive a mean, practical value for the Weber-Fechner fraction. It is also of practical significance to derive an average curve for the relationship between the contrast difference ΔC and the base contrast C . This was achieved by taking data for a target size of 0.15deg at a luminance of $28\text{cd}\cdot\text{m}^{-2}$ as the standard. Data for other conditions were then adjusted by eye to produce a best fit to the standard. This adjustment was made by moving each data set along a 45deg line so that both contrast and contrast difference are scaled by the same factor. The results of this process are shown for the two observers in Figures

8a6b. These scatter plots were then averaged in bins of width 0.2 lu (log unit) along the abscissa to yield the square symbols shown in Figure 8c. The crosses and dashed line in Figure 8c represent a theoretical function as described in the Discussion (Section 4).

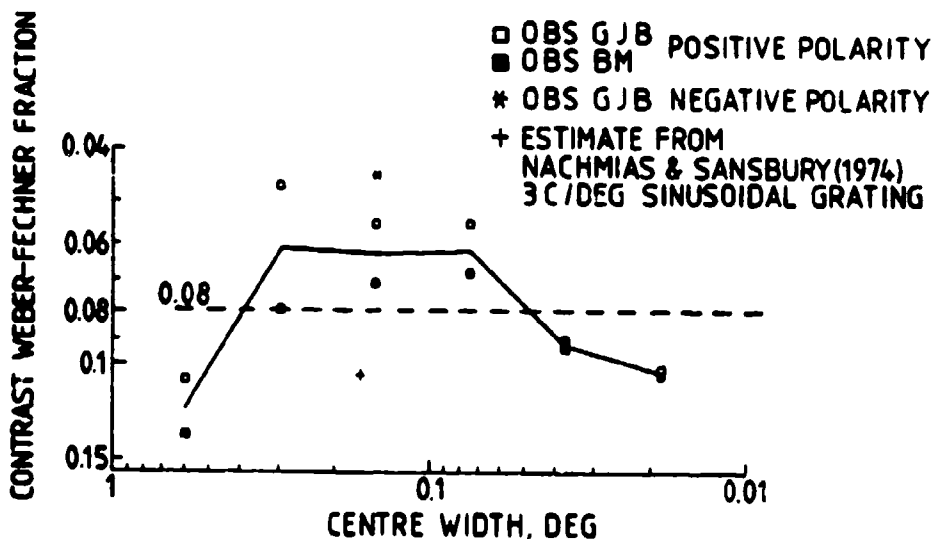


FIG 7 Estimates of the Weber-Fechner fraction obtained from contrast discrimination data for base contrasts in excess of the conventional threshold value. Filled and open squares are values for Observers EM (data from Fig 4a) and GJB (data for Fig 4b) respectively. The fraction obtained for negative triphasic targets (Fig 3b) is indicated by the asterisk. The cross shows the estimate obtained from data given by Nachmias and Sansbury (Ref 35): it is plotted against the equivalent triphasic bar width. A mean value for all target widths and observers is indicated by the dashed line at a value of the contrast Weber-Fechner fraction equal to 0.08.

Up to this point the values of contrast difference have been determined at only the 71% level of discrimination. For purposes of theoretical analysis and practical application it is crucial to determine how the probability of discrimination varies with values of contrast difference. For conventional threshold values the psychometric function is approximately constant when plotted on a normalised scale in which the contrasts are divided by the contrast appropriate to some fixed probability (Refs 41, 42). There are only minor differences between this representation and the one in which the scale is represented by log contrast (Ref 43). For the contrast discrimination experiments it is not immediately obvious whether the scale variable should be the contrast, $C + \Delta C$, of the adjustable stimulus, the contrast difference ΔC , or some other function of C and ΔC . In order to identify the appropriate transformation, psychometric functions were determined for a triphasic target of fixed width 0.15deg and luminance 28cd.m^{-2} . Three values of base contrast C were chosen: $C=0$, 0.03 and 0.2. The first value corresponds to the conventional threshold, the second is just within the contrast Weber-Fechner region and the third is towards the end of this region (Fig 3). Probability values are shown in Figure 9. They were estimated from an

UNCLASSIFIED

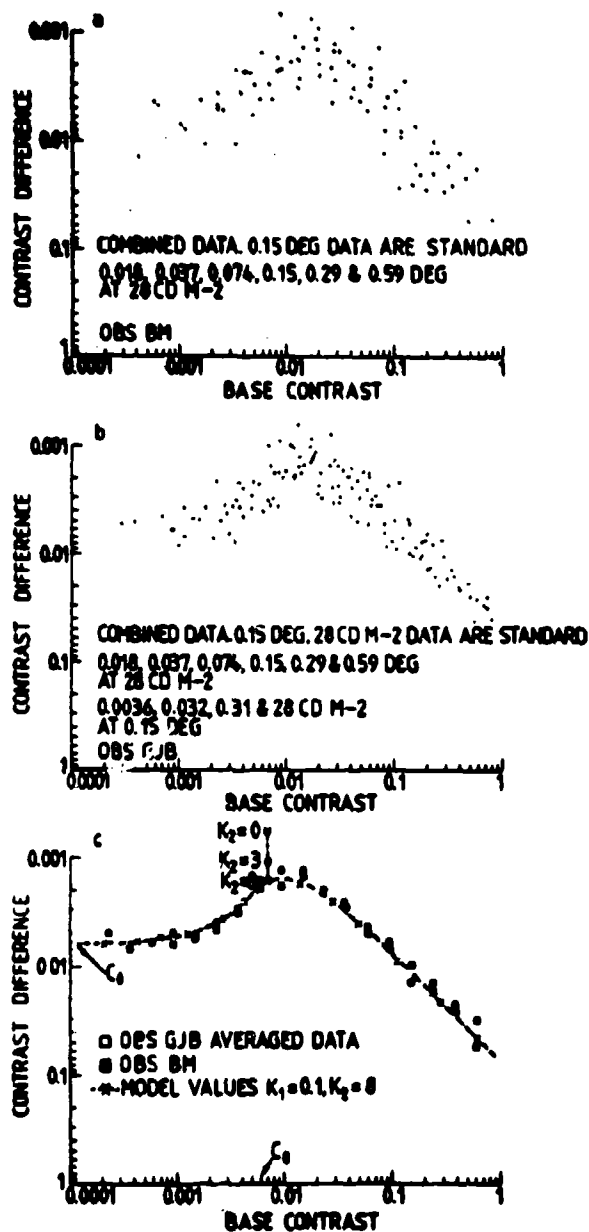


FIG 8 Combined data of contrast discrimination for triphasic targets versus base contrast obtained by scaling both coordinates by the same amount in order to produce a satisfactory fit to data for target width 0.15deg and luminance 28cd.m⁻².

- (a) Observer BM.
- (b) Observer GJB. The combined values are indicated in the legend and were obtained from Figs 4a&b & 5.
- (c) Squares show averaged contrast discrimination data obtained from (a) and (b). Filled and open squares represent mean values for Observers BM and GJB respectively. The crosses and broken line give the theoretical function as described in the Annex. This function was fitted to the experimental data by setting the conventional contrast threshold level equal to 0.006, $K_1=0.1$ and $K_2=8$. The value of K_1 produces a contrast Weber-Fechner fraction of 0.08. The asterisks show sequential calculations obtained as K_1 was held constant at 0.1 and K_2 was increased from zero until satisfactory agreement occurred with the experimental data.

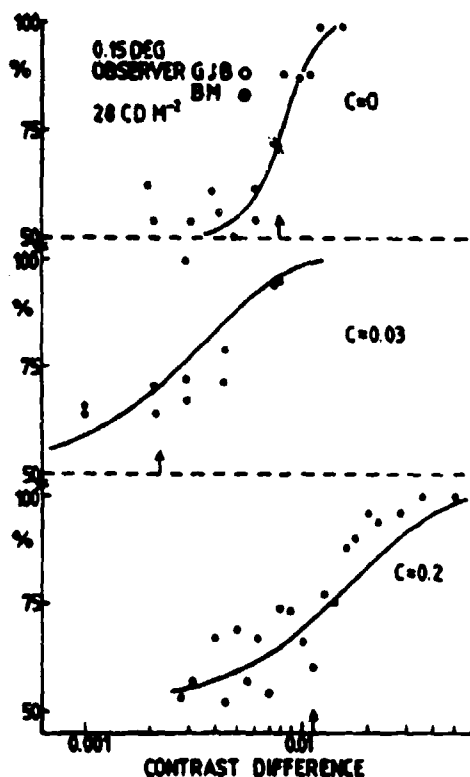


FIG 9 Psychometric functions obtained by determining the probability of contrast discrimination as a function of contrast difference. The method of side-by-side forced-choice was used for positive, triphasic targets. Values are shown for three base contrasts: $C=0$, 0.03 and 0.2 . Filled circles and open circles show data for Observers BM and GJB respectively. Each value of probability is based on approximately 40 presentations per point. Continuous lines show theoretical calculations obtained by the method described in the Annex. The arrow on each abscissa indicates the contrast difference required for a probability of contrast discrimination equal to 71%. Target width 0.15deg , luminance $28\text{cd}\cdot\text{m}^{-2}$.

average of about 40 presentations per point. The continuous lines are calculated from the theoretical derivation given in the Annex. The arrows on the abscissa denote values of contrast difference giving probabilities of 0.71. Note that the psychometric function for zero base contrast is steeper than those for base contrasts within the contrast Weber-Fechner region.

4 DISCUSSION

Contrast discrimination has been measured for triphasic targets of different widths (Fig 4), polarities (Fig 3b), aspect ratios (Fig 6) and

UNCLASSIFIED

luminances (Fig 5). Overall, the results can be efficiently described by a single curve of contrast difference ΔC against base contrast C with the condition that both ΔC and C are scaled by a constant, determined only by the conventional threshold level. The value of conventional threshold in particular can be manipulated either by changing the target width or by changing the luminance. The standard curve (Fig 8c) can be fitted approximately to all sets of data of ΔC against C by the choice of an appropriate scaling constant which is applied to both axes. This description of contrast discrimination is sufficiently accurate for many practical purposes, but it must be remembered that it is not precise since repetitive experimentation can yield variations in the contrast Weber-Fechner fraction with different target widths (Fig 7).

For base contrasts C somewhat less than the conventional threshold level C_0 (Fig 8c), the results are accurately described by the equation:

$$C + \Delta C = C_0; C/C_0 < 0.6 \quad (4)$$

The linear relationship between ΔC and C in the region of subthreshold addition confirms previous investigations (Refs 6, 44) and follows logically if the existence of both small-signal linearity and a neural threshold device are assumed. If no such device exists, then a non-linearity in the form of an accelerating function (eg a quadratic dependence of output on input contrast) is postulated (Ref 35) in order to provide values of ΔC which decrease with increasing (small) values of C . For the purposes of the present analysis the existence of neural threshold devices is assumed since such mechanisms provide a parsimonious description of the experimental results of subthreshold addition.

For base contrasts C somewhat greater than the conventional threshold level C_0 , contrast discrimination follows a Weber-Fechner relationship in the contrast domain:

$$\Delta C = W.C; C/C_0 > 3 \quad (5)$$

An equation of this form can arise, for example, from a logarithmic transducer function with a constant noise level added after the non-linearity. However, perceived contrast seems to be equal to actual contrast minus contrast threshold (Refs 9, 10). Even though this (linear) transducer function could be the result of cascading two or more non-linear functions (Ref 45), the simpler assumption of linearity at each stage has been made in the present analysis. In order to reproduce the contrast Weber-Fechner relationship of equation 5, it is therefore necessary to include a noise process with a magnitude which is proportional to the contrast (signal) level. In addition another noise process must be included which has a level proportional to the conventional threshold level C_0 ; ie a constant noise level for a given target. This further noise source is needed in order to prevent the derived psychometric functions from becoming extremely steep at low base contrasts, especially when plotted against log contrast difference $\log \Delta C$. The two noise sources are assumed to be uncorrelated and have Gaussian probability distributions (Fig 10b). The noise levels can therefore be described by equivalent standard deviations σ . For the first noise process set the noise level σ_1 by:

$$\sigma_1 = K_1.C \quad (6)$$

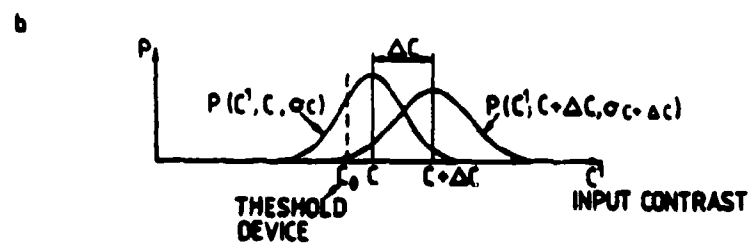
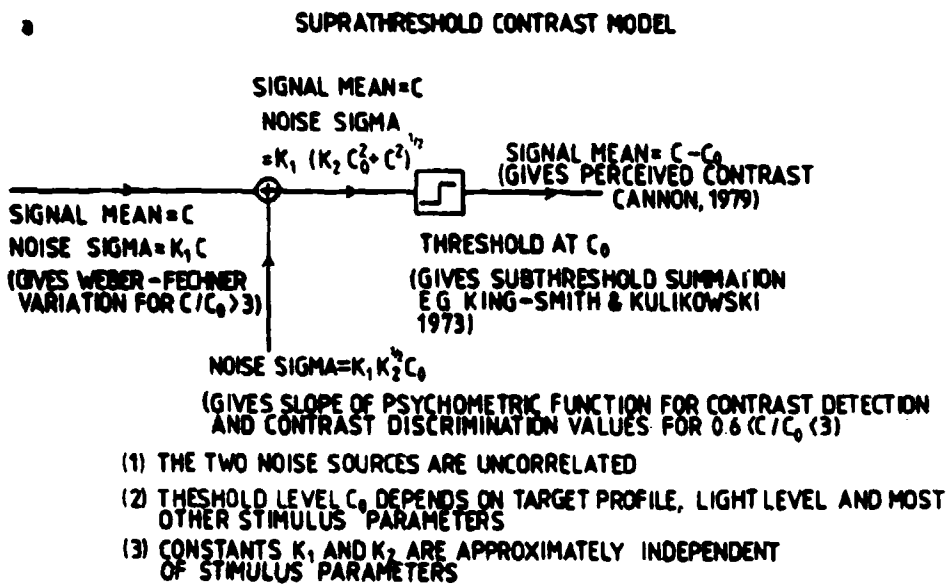


FIG 10 The suprathreshold contrast model used to derive theoretical estimates of contrast discrimination (see Annex).
(a) Shows the schematic modelling illustrating interactions of signal, noise and the threshold device.
(b) Probabilistic responses to target contrasts C and $C + \Delta C$. The dashed line indicates the contrast level set by the threshold device. All response values are related to equivalent input contrast levels.

and for the second noise process set:

$$\sigma_2 = K_1 \cdot K_2^{1/2} \cdot C_0 \tag{7}$$

where K_1 and K_2 are approximately independent of stimulus parameters such as size and luminance. The conventional threshold contrast is C_0 . The combined noise level from the two uncorrelated sources is then:

$$\sigma = (\sigma_1^2 + \sigma_2^2)^{1/2} = K_1 \cdot (K_2 \cdot C_0^2 + C^2)^{1/2},$$

and when scaled with respect to C_0 is:

UNCLASSIFIED

$$S_T = K_1 \cdot (K_2 + T^2)^{\frac{1}{2}} \quad (8)$$

where $S_T = \sigma / C_0$

and $T = C / C_0$

A model was devised both to describe the contrast discrimination data and to be consistent with subthreshold summation data. It is shown schematically in Figure 10a. Many such arrangements can be used within the components of multiple-channel models (Refs 4, 25) and for separate processing of different contrast polarities (Refs 46, 47). Such parallel processing is not described specifically in the present analysis: it is assumed only that some unspecified process defines the conventional threshold level C_0 . An equation is derived in the Annex which gives the probability of discriminating targets of contrasts C and $C + \Delta C$ in terms of the conventional threshold level C_0 and the constants K_1 and K_2 . The average value of the contrast Weber-Fechner fraction W in equation 5 is taken as 0.08 (Fig 7). This fixes the value of K_1 at 0.1 (Annex). The value of K_2 was then adjusted stepwise until the theoretical variation of ΔC with C gave satisfactory agreement with the experimental data (Fig 8c). The value chosen for K_2 is 8. Note that if only one parameter, K_1 , is used (ie $K_2=0$), the maximum enhancement in sensitivity over the conventional threshold level (Fig 8c) is over 1 lu, whereas the experimental data indicates about 0.6 lu. In addition and as noted earlier, very steep psychometric functions occur as the base contrast C becomes small. The complete theoretical variation of ΔC with C is shown by the crosses and dashed line in Figure 8c. As the base contrast becomes small the discrimination process tends towards that for conventional threshold levels. The psychometric function is then simply the cumulative (error) function derived from the second noise process (equation 7 and Annex). Therefore

$$\sigma / C_0 = K_1 \cdot K_2^{\frac{1}{2}} = 0.28 \quad (9)$$

This value of σ / C_0 compares favourably with independent and direct estimates produced by other authors. For example, Blackwell (Ref 42) derived values in the range 0.314 to 0.584 from data obtained by 36 observers.

An example of practical application of the contrast discrimination model is now considered. As discussed in the Introduction, there is an interaction between spatial frequency and the number of detectable contrast steps (grey scale). This can be easily appreciated by considering the detection of a fine grating which has a spatial frequency approaching the resolution limit. At such high frequencies only zero contrast and a contrast of one need to be represented. The required number of contrast steps is therefore some function of the conventional threshold level C_0 . However, contrast discrimination ΔC is clearly not equal to C_0 , irrespective of the base contrast C as assumed, for example, by Roetling (Ref 29).

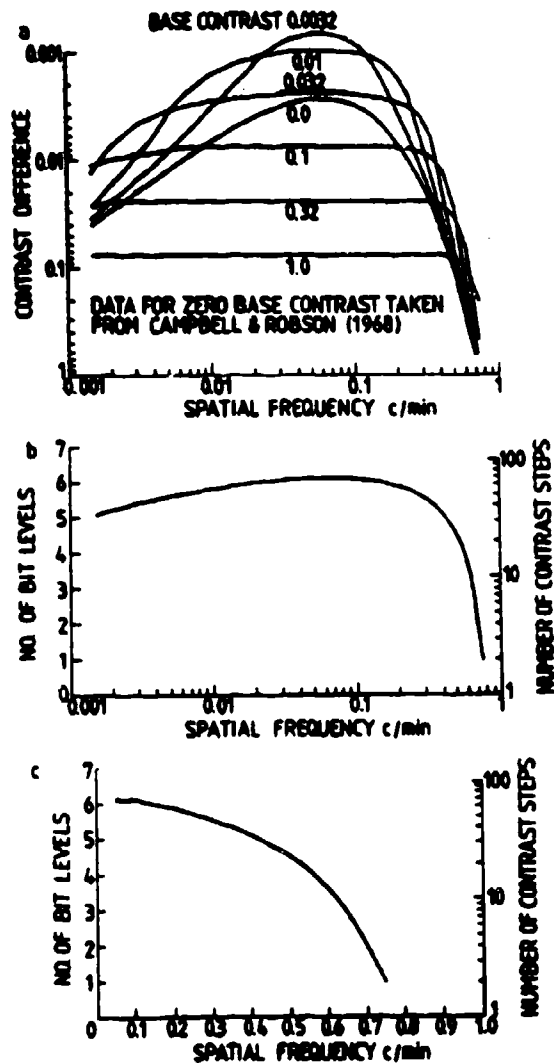


FIG 11 Theoretical calculations obtained using equation 19 (Annex).
 (a) Generalised contrast sensitivity functions. Each curve illustrates the contrast difference, as a function of spatial frequency, obtained for a fixed level of base contrast. Values of base contrast are shown adjacent to the corresponding curves. Data for zero base contrast, is the conventional contrast threshold levels, are taken from Campbell & Robson (Ref 4).
 (b) Number of discriminable contrast steps calculated as a function of log. spatial frequency. The number of steps is also represented on a base 2 logarithmic scale.
 (c) As (b) except that spatial frequency is represented on a linear scale.

UNCLASSIFIED

On the basis of the relationship between ΔC and C given in Figure 8c, the contrast sensitivity function for sinusoidal gratings can be generalised to give contrast difference functions. The contrast threshold (ie the conventional threshold level C_0) is not determined as a function of spatial frequency; instead the contrast is fixed at some level C , and values of ΔC are determined as a function of spatial frequency. Different values of C then produce different curves of ΔC against frequency. Conventional contrast threshold values were obtained by fitting a smooth curve through data given by Campbell & Robson (Ref 4). The curve was used to produce the generalised contrast sensitivity functions shown in Figure 11a. The corresponding required number of contrast steps at different spatial frequencies is plotted in Figure 11b on a log frequency scale and in Figure 11c on a linear frequency scale. Each value was calculated by counting the number of contrast discrimination steps from the conventional threshold level up to a contrast of 1.0. The values are also shown on a base 2 logarithmic scale in order to illustrate the number of bits required at each spatial frequency. Note in particular that the number of bit levels is greatly reduced at medium to high spatial frequencies. The curves shown in Figure 11a illustrate that care must be exercised when applying contrast sensitivity functions (conventional threshold values, $C=0$) to suprathreshold situations. For example, the process of recognition of real objects often requires the detection of features within the objects which are themselves superimposed on other, suprathreshold features. In addition calculations of the number of detectable contrast steps (Figs 11b&c) suggest that novel and efficient ways of image coding may be possible which produce no detectable changes in the image when subsequently decoded. Finally, improved signal transfer functions can be devised for imaging systems which use some intermediate digital storage.

5 CONCLUSIONS

- a) The just-noticeable-difference (JND) in contrast of targets, localised in both space and spatial frequency, is approximately 8% when the target itself is detectable.
- b) The function describing the variation of JND with contrast level is approximately invariant for wide ranges of experimental conditions, provided that both variables are scaled with respect to the conventional target threshold level.
- c) The results can be applied immediately to the specification of just detectable changes in imaging system MTF and to the required accuracy in the measurement of MTF.
- d) The experimental results and theoretical description provide a firm basis for the construction of visual models applicable to the prediction of the detectability of changes in imaging system parameters or designs, and to the detection of targets or features within targets, especially when presented on structured background fields.

UNCLASSIFIED

6 REFERENCES

- 1 Schade O Optical and Photoelectric Analog of the Eye. J Opt Soc Amer 46, 721-739 (1956).
- 2 Davidson M Perturbation Approach to Spatial Brightness Interaction in Human Vision. J Opt Soc Amer 58, 1300-1308 (1968).
- 3 Campbell F W, Carpenter R H S, & Levinson J Z Visibility of Aperiodic Patterns Compared with that of Sinusoidal Gratings. J Physiol (Lond) 204, 283-298 (1969).
- 4 Campbell F W, & Robson, J G Application of Fourier Analysis to the Visibility of Gratings. J Physiol (Lond) 197, 551-556 (1968).
- 5 Blakemore, C Campbell FW On the Existence of Neurones in the Human Visual System Selectivity Sensitive to the Orientation and Size of Retinal Images. J Physiol (Lond) 203, 237-260 (1969).
- 6 Kulikowski J J, King-Smith P E Spatial Arrangement of Line, Edge and Grating Detectors Revealed by Subthreshold Summation. Vision Res 13, 1455-1478 (1973).
- 7 Hauske G, Wolf W, & Lupp U Matched Filters in Human Vision. Biol Cybernetics 22, 181-188 (1976).
- 8 Georgeson M A, Sullivan G D Contrast Constancy: Deblurring in Human Vision by Spatial Frequency Channels. J Physiol (Lond) 252, 627-656 (1975).
- 9 Kulikowski J J Effective Contrast Constancy and Linearity of Contrast Sensation. Vision Res 16, 1419-1431 (1976).
- 10 Cannon M W Contrast Sensation: A Linear Function of Stimulus Contrast. Vision Res 19, 1045-1052 (1979).
- 11 Bryngdahl O Characteristics of the Visual System: Psychophysical Measurements of the Response to Spatial Sine-Wave Stimuli in the Photopic Region. J Opt Soc Amer 56, 811-821 (1966).
- 12 Watanabe A, Mori T, Nagata S, & Hiwatashi K Spatial Sine-Wave Responses of the Human Visual System. Vision Res 8, 1245-1263 (1968).
- 13 Blakemore C, Muncey J P J, & Ridely, R M Stimulus Specificity in the Human Visual System. Vision Res 13, 1915-1931 (1973).
- 14 Snyder A W, & Srinivasan M V Human Psychophysics: Functional Interpretation for Contrast Sensitivity Versus Spatial Frequency Curve. Biol Cybernetics 32, 9-17 (1979).
- 15 Hall C F, Hall E L A Non-Linear Model for the Spatial Characteristics of the Human Visual System. IEEE Trans on Systems, Man & Cyber SMO-7, 161-170 (1977).
- 16 Enroth-Ogell C, & Robson J G The Contrast Sensitivity of Retinal Ganglion Cells of the Cat. J Physiol (Lond) 187, 517-552 (1966).
- 17 Maffei L, Fiorentini A Retinogeniculate Convergence and Analysis of Contrast. J Neurophysiol 35, 65-86 (1972).

UNCLASSIFIED

- 18 Maffei, L The Visual Cortex as a Spatial Frequency
Florentini A Analyser. Vision Res 13, 1255-1267 (1973).
- 19 Kozak W M, Color-Dependent Distribution of Spikes in
Reitboeck H J Single Optic Tract Fibres of the Cat.
Vision Res 14, 405-419 (1974).
- 20 Pollehn H, & Effect of Noise on the Modulation Transfer
Roehrig H Function of the Visual Channel. J Opt Soc
Amer 60, 842-848 (1970).
- 21 Stromeyer C F, Spatial-Frequency Masking in Vision: Critical
Julesz B Bands and Spread of Masking. J Opt Soc Amer
62, 1221-1232 (1972).
- 22 MacLeod I D G, The Visibility of Gratings: Spatial Frequency
Rosenfeld A Channels or Bar-Detecting Units ? Vision Res
14, 909-915 (1975).
- 23 Burton G J Visual Detection Model for Static Targets.
Paper Presented to Symposium on Modelling for
Operational Research, Royal Military College
of Science, Shrivenham, UK. January 1978.
- 24 Wilson H R, A Four Mechanism Model for Threshold Spatial
Bergen J R Vision. Vision Res 19, 19-23 (1979).
- 25 Bergen J R, Further Evidence for Four Mechanisms Mediating
Wilson H R, Vision at Threshold: Sensitivities to Complex
Cowan J D Gratings and Aperiodic Stimuli. J Opt Soc Amer
69, 1580-1587 (1979).
- 26 Marr D Early Processing of Visual Information. Proc
Roy Soc B, 275, 483-519 (1976).
- 27 Charman W N, Accommodation as a Function of Object Form.
Tucker J Am J Optom and Physiol Opt (USA) 55, 84-92
(1978).
- 28 Judice C N, Using Ordered Dither to Display Continuous Tone
Jarvis J F, Pictures on an AC Plasma Panel. Proc SID 15,
Ninke W H 161-169 (1974).
- 29 Roetling P G Visual Performance and Image Coding. Proc SID
17, 111-114 (1976).
- 30 Mezrich J J, Image Descriptors for Displays. RCA Labs,
Carlson, C R, Princeton, NJ 08540, USA. Contract No N00014-
Cohen R W 74-C-0184. (Feb 1977).
- 31 Hall C F, Digital Colour Image Compression in a Percep-
Andrews H C tual Space. Proc SPIE 149, 182-188 (1978).
- 32 Pratt W K Digital Image Processing. J Wiley & Sons, NY
(1978).
- 33 King-Smith P E, The Detection of Gratings by Independent
Kulikowski J J Activation of Line Detectors. J Physiol (Lond)
247, 237-271 (1975).
- 34 Graham N, Grating Summation in Fovea and Periphery.
Robson J G, Vision Res 18, 815-825 (1978).
- 35 Nachmias J, Grating Contrast: Discrimination May be Better
Nachmias J, Than Detection. Vision Res 14, 1039-1042 (1974).
- 36 Sansbury R V Contrast-Difference Thresholds With Sinusoidal
Kohayakawa Y Gratings. J Opt Soc Amer 62, 584-587 (1972).
- 37 Crawford B H Notes on Applied Science Series "Physical
Photometry". HMSO (Lond) No 29 (1962).

UNCLASSIFIED

- 38 Cornsweet T N The Staircase-Method in Psychophysics. Am J Psychol 75, 485-491 (1962).
- 39 Kelly D H, Savoie R E A Study of Sine-Wave Contrast Sensitivity by Two Psychophysical Methods. Perception & Psychophysics 14, 313-318 (1973).
- 40 Campbell F W, Kulikowski J J Orientational Selectivity of the Human Visual System. J Physiol (Lond) 187, 437-445 (1966).
- 41 Blackwell H R Contrast Thresholds of the Human Eye. J Opt Soc Amer 36, 624-643 (1946).
- 42 Blackwell H R Neural Theories of Simple Visual Discriminations. J Opt Soc Amer 53, 129-160 (1963).
- 43 Nachmias J Effect of Exposure Duration on Visual Contrast Sensitivity With Square-Wave Gratings. J Opt Soc Amer 57, 421-427 (1967).
- 44 Kulikowski J J, Abadi R, King-Smith P E Orientational Selectivity of Grating and Line Detectors in Human Vision. Vision Res 13, 1479-1486 (1973).
- 45 Cornsweet T Visual Perception. Academic Press, New York (1970).
- 46 de Valois K K Independence of Black and White: Phase-Specific Adaptation. Vision Res 17, 209-215 (1977).
- 47 Burton G J, Nagshineh S, Ruddock K H Processing by the Human Visual System of the Light and Dark Contrast Components of the Retinal Image. Biol Cybernetics 27, 189-197 (1977).

REPORTS OF THE COMMITTEE ARE NOT AVAILABLE IN
 A SEPARATE FORM. MEMBERS OF THE COMMITTEE
 SHOULD CONTACT THE ORGANISATION

THEORETICAL MODEL OF CONTRAST DISCRIMINATION

Assume that the noise processes generate Gaussian probability density distributions when referred back to input contrast levels. Thus, an input of contrast C_m produces an output which at some time and with probability $P(C'; C_m, \sigma) dC'$ is identical to an input of contrast C' where:

$$P(C'; C_m, \sigma) = (1/\sigma\sqrt{2\pi}) \cdot \exp[-(C' - C_m)^2 / 2\sigma^2] \quad (10)$$

Two targets, contrasts C and $C + \Delta C$, generate the two probability density distributions shown in Figure 10b. The dashed line at contrast C_0 represents the threshold device. Responses which correspond to input contrasts below C_0 are not transmitted through the threshold device. The forced-choice experiments determine the probability that a target of contrast, $C + \Delta C$, is correctly assigned as being of higher contrast than one of contrast C for $\Delta C > 0$. This probability function is composed of three parts. Firstly, the following equation gives the probability P_1 that both targets are detected and also that a correct choice of target is made.

$$P_1 = \int_{C_0}^{\infty} P(C'; C, \sigma_C) \int_{C'}^{\infty} P(C''; C + \Delta C, \sigma_{C + \Delta C}) \cdot dC'' \cdot dC' \quad (11)$$

Secondly, the probability P_2 that the target of contrast C is not detected but that of contrast, $C + \Delta C$, is detected is:

$$P_2 = \int_{-\infty}^{C_0} P(C'; C, \sigma_C) \cdot dC' \cdot \int_{C_0}^{\infty} P(C'; C + \Delta C, \sigma_{C + \Delta C}) \cdot dC' \quad (12)$$

This again corresponds to the probability of a correct choice. Thirdly, the probability P_3 that both targets are not detected and a correct choice is made by guessing is:

$$P_3 = \frac{1}{2} \int_{-\infty}^{C_0} P(C'; C, \sigma_C) \cdot dC' \cdot \int_{-\infty}^{C_0} P(C'; C + \Delta C, \sigma_{C + \Delta C}) \cdot dC' \quad (13)$$

For all conditions the probability P^+ of a correct choice is the sum

$$P^+ = P_1 + P_2 + P_3 \quad (14)$$

$$\text{Using } \text{erf}(x) = (2/\sqrt{\pi}) \cdot \int_0^x \exp(-y^2) \cdot dy \quad (15)$$

$$\text{then } \int_x^{\infty} P(C'; C_m, \sigma) \cdot dC' = \frac{1}{2} \cdot [1 - \text{erf}(\frac{x - C_m}{\sqrt{2}\sigma})] \quad (16)$$

UNCLASSIFIED

and equation 14 can be rearranged to yield:

$$P^+ = \frac{1}{2} + \frac{1}{8} \cdot \left[\frac{1 + \operatorname{erf}\left(\frac{C_0 - C}{\sqrt{2}\sigma_C}\right)}{\sqrt{2}\sigma_C} \right] \cdot \left[\frac{1 - \operatorname{erf}\left(\frac{C_0 - C - \Delta C}{\sqrt{2}\sigma_{C+\Delta C}}\right)}{\sqrt{2}\sigma_{C+\Delta C}} \right]$$

$$- \frac{1}{2} \cdot \frac{1}{\sqrt{2\pi}\sigma_C} \cdot \int_{C_0}^{\infty} \exp\left[-(C' - C)^2 / 2\sigma_C^2\right] \cdot \operatorname{erf}\left(\frac{C' - C - \Delta C}{\sqrt{2}\sigma_{C+\Delta C}}\right) dC' \quad (17)$$

Scale all contrast terms with respect to C_0 by setting:

$$T = C / C_0$$

$$\Delta T = \Delta C / C_0$$

$$S_T = \sigma_C / C_0$$

$$S_{T+\Delta T} = \sigma_{C+\Delta C} / C_0 \quad (18)$$

and $S_{T+\Delta T} = \sigma_{C+\Delta C} / C_0$

Then:

$$P^+ = \frac{1}{2} + \frac{1}{8} \cdot \left[\frac{1 + \operatorname{erf}\left(\frac{1 - T}{\sqrt{2}S_T}\right)}{\sqrt{2}S_T} \right] \cdot \left[\frac{1 - \operatorname{erf}\left(\frac{1 - T - \Delta T}{\sqrt{2}S_{T+\Delta T}}\right)}{\sqrt{2}S_{T+\Delta T}} \right]$$

$$- \frac{1}{2} \cdot \frac{1}{\sqrt{2\pi}S_T} \cdot \int_1^{\infty} \exp\left[-(x - T)^2 / 2S_T^2\right] \cdot \operatorname{erf}\left(\frac{x - T - \Delta T}{\sqrt{2}S_{T+\Delta T}}\right) \cdot dx \quad (19)$$

From equation 8:

$$S_T = K_1 \cdot [K_2 + T^2]^{\frac{1}{2}}$$

and (20)

$$S_{T+\Delta T} = K_1 \cdot [K_2 + (T + \Delta T)^2]^{\frac{1}{2}}$$

The probability of correct discrimination P^+ is dependent only upon values of contrast which are scaled with respect to C_0 , the conventional threshold value. If K_1 and K_2 are independent of C_0 , then the curve of log contrast difference $\log \Delta C$ versus log base contrast $\log C$ for a given probability of discrimination has a fixed shape and can be adjusted for targets having different values of C_0 by sliding along a 45deg line as described in Section 3.

The theoretical curve of ΔC against C shown in Figure 8c, was produced by solving equation 19 numerically for a given value of T and adjusting ΔT in a systematic manner until P^+ equalled 0.707. Theoretical probability of discrimination values shown in Figure 9 were generated for a given value of T by a straightforward numerical solution of equation 19 with different values of ΔT , each value yielding a corresponding probability P^+ .

UNCLASSIFIED

Appropriate values for the constants K_1 and K_2 in equation 20 were selected separately. For large T , S_T is approximately equal to $K_1 T$. Therefore, the constant K_1 can be obtained from equation 19 with the condition that $\Delta C/C$, and hence $\Delta T/T$, is equal to 0.08, the mean value of the contrast Weber-Fechner fraction (Fig 7). The value of K_2 was then increased from zero for $C/C_0 = T = 1$, as shown by the asterisks in Figure 8c, until satisfactory agreement was obtained with the experimental data.

DOCUMENT CONTROL SHEET
(Notes on completion overleaf)

Overall security classification of sheet **UNCLASSIFIED**

(As far as possible this sheet should contain only unclassified information. If it is necessary to enter classified information, the box concerned must be marked to indicate the classification eg (R),(C) or (S)).

1. DRIC Reference (if known)	2. Originator's Reference RADE Technical Report 2/81	3. Agency Reference	4. Report Security Classification Unclassified
5. Originator's Code (if known) 851600	6. Originator (Corporate Author) Name and Location Ministry of Defence Royal Armament Res and Dev Est		
5a. Sponsoring Agency's Code (if known)	6a. Sponsoring Agency (Contract Authority) Name and Location		
7. Title Contrast Discrimination by the Human Visual System			
7a. Title in Foreign Language (in the case of translations)			
7b. Presented at (for conference papers). Title, place and date of conference			
8. Author 1. Surname, initials Burton G J	9a Author 2	9b Authors 3, 4...	10. Date pp ref May '81 26 47
11. Contract Number	12. Period	13. Project	14. Other References
15. Distribution statement No Limitations			
Descriptors (or keywords) Vision Contrast discrimination Imaging systems Modulation transfer function			
continue on separate piece of paper if necessary			
Abstract In vision of everyday scenes features requiring detection are frequently observed in the presence of suprathreshold background structures. Detection of such features is a contrast discrimination task and is often necessary for the subsequent process of recognition. In order to provide a description of this task, contrast discrimination measurements were determined for targets with luminance profiles which were localised in both space and spatial frequency. The investigation extends earlier work on this topic by measurement of contrast discrimination levels for different base contrasts, sizes, luminances and aspect ratios of the targets. A model is proposed to describe the contrast discrimination process, and an example is given of a simple application of the model to the determination of the number of discriminable steps in contrast as a function of the spatial frequency of a sinusoidal grating target.			

UNCLASSIFIED

62.843.3

Ministry of Defence

Royal Armament Research and Development Establishment

RADE Technical Report 2/81

UNCLASSIFIED

62.843.3

Ministry of Defence

Royal Armament Research and Development Establishment

RADE Technical Report 2/81

UNCLASSIFIED

May 1981

G J Burton

UNCLASSIFIED

May 1981

G J Burton

In vision of everyday scenes features requiring detection are frequently observed in the presence of suprathreshold background structures. Detection of such features is a contrast discrimination task and is often necessary for the subsequent process of recognition. In order to provide a description of this task, contrast discrimination measurements were determined for targets with luminance profiles which were localised in both space and spatial frequency. The investigation extends earlier work on this topic by measurement of contrast discrimination levels for different base contrasts, sizes, luminances and aspect ratios of the targets. A model is proposed to describe the contrast discrimination process, and an example is given of a

In vision of everyday scenes features requiring detection are frequently observed in the presence of suprathreshold background structures. Detection of such features is a contrast discrimination task and is often necessary for the subsequent process of recognition. In order to provide a description of this task, contrast discrimination measurements were determined for targets with luminance profiles which were localised in both space and spatial frequency. The investigation extends earlier work on this topic by measurement of contrast discrimination levels for different base contrasts, sizes, luminances and aspect ratios of the targets. A model is proposed to describe the contrast discrimination process, and an example is given of a

UNCLASSIFIED

62.843.3

Ministry of Defence

Royal Armament Research and Development Establishment

RADE Technical Report 2/81

UNCLASSIFIED

62.843.3

Ministry of Defence

Royal Armament Research and Development Establishment

RADE Technical Report 2/81

UNCLASSIFIED

May 1981

G J Burton

UNCLASSIFIED

May 1981

G J Burton

In vision of everyday scenes features requiring detection are frequently observed in the presence of suprathreshold background structures. Detection of such features is a contrast discrimination task and is often necessary for the subsequent process of recognition. In order to provide a description of this task, contrast discrimination measurements were determined for targets with luminance profiles which were localised in both space and spatial frequency. The investigation extends earlier work on this topic by measurement of contrast discrimination levels for different base contrasts, sizes, luminances and aspect ratios of the targets. A model is proposed to describe the contrast discrimination process, and an example is given of a

In vision of everyday scenes features requiring detection are frequently observed in the presence of suprathreshold background structures. Detection of such features is a contrast discrimination task and is often necessary for the subsequent process of recognition. In order to provide a description of this task, contrast discrimination measurements were determined for targets with luminance profiles which were localised in both space and spatial frequency. The investigation extends earlier work on this topic by measurement of contrast discrimination levels for different base contrasts, sizes, luminances and aspect ratios of the targets. A model is proposed to describe the contrast discrimination process, and an example is given of a

UNCLASSIFIED

UNCLASSIFIED